A HIGHLY ACCURATE SPHERICAL NEAR-FIELD ARCH POSITIONING SYSTEM

Jeffrey Fordham, Tim Schwartz, George Cawthon, Youlian Netzov, Scott McBride,
Makary Awadalla, Dave Wayne

MI Technologies
1125 Satellite Boulevard, Suite 100
Suwanee, Georgia 30024, USA

ABSTRACT

Highly accurate spherical near-field measurement systems require precise alignment of the probe antenna to the measurement surface. MI Technologies has designed and constructed a new spherical near field arch positioner with a 1.5 meter radius to support measurements requiring accurate knowledge of the probe phase center to within .0064 cm throughout its range of travel.

To achieve this level of accuracy, several key design elements were considered. First, a highly robust mechanical design was considered and implemented. Second, a tracking laser interferometer system was included in the system for characterization of residual errors in the position of the probe. Third, a position control system was implemented that would automatically correct for the residual errors.

The scanner includes a two position automated probe changer for automated measurements of multi-band antennas and a high accuracy azimuth axis. The azimuth axis includes an algorithm for correcting residual, repeatable positioning errors.

This paper defines the spherical near-field system and relation of each axis to the global coordinate system, discusses their associated error sources and the effect on global positioning and presents achieved highly accurate results.

Keywords: Spherical Near-Field, Probe, Arch Positioner

1. Introduction

Since its introduction in the 1970's Spherical Near-Field (SNF) antenna measurements has become a method of choice for high accuracy. Much has been written and published in the literature about SNF antenna measurements, most notably J.E. Hansen's book [1]. As the state-of-the-art antenna design has progressed, so has the need for state-of-the-art measurement systems to characterize complex antennas.

Complex antennas require characterization of element patterns and excitations, boresight requirements and extremely accurate sidelobe level measurements [2]. In order to create measurement systems to address these needs extra care must be placed on all aspects of the measurement system design to ensure accuracy. Care must be taken in the design of the RF subsystem to control stability and accuracy, the facility must be designed to minimize thermal effects, the probes used in the measurement must be characterized and mechanical accuracy of the positioning system must be addressed. As the complexity of the antennas has increased so has the operational frequency of the antennas increased. The increase in frequency adds additional requirements to the accuracy of the mechanical positioning devices required to move the probe and antenna under test (AUT) in order to minimize phase errors in the measurement.

To address the accuracy concerns of the mechanical positioners, advanced installation and alignment techniques have been designed and implemented including the use of tracking laser interferometers to align SNF measurement systems [3]. The tracking lasers have been used in PNF measurements [4] as well as SNF measurements [5] to provide an error map of residual alignment errors and correct for position errors on the fly.

Several systems using a circular arc with a travelling probe carriage have been designed and constructed to deliver high performance [2, 4, 5, 6] mechanical accuracy for demanding antenna measurements. These arches, already reported in the literature, have radii of 5 and 10 meters for testing large articles. This paper reports on another SNF positioning system based on an arch with a design radius of 1.5 meters and position accuracies that will support smaller test objects and millimeter wave frequency measurements. Figure 1 shows a CAD model of the measurement system.

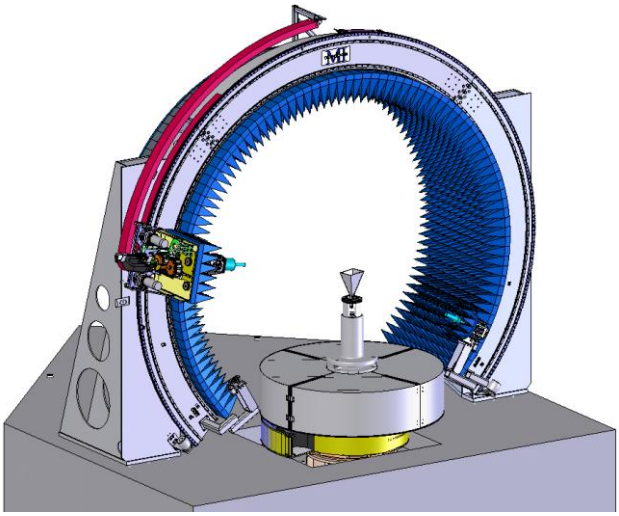

Figure 1 – SNF Measurement System

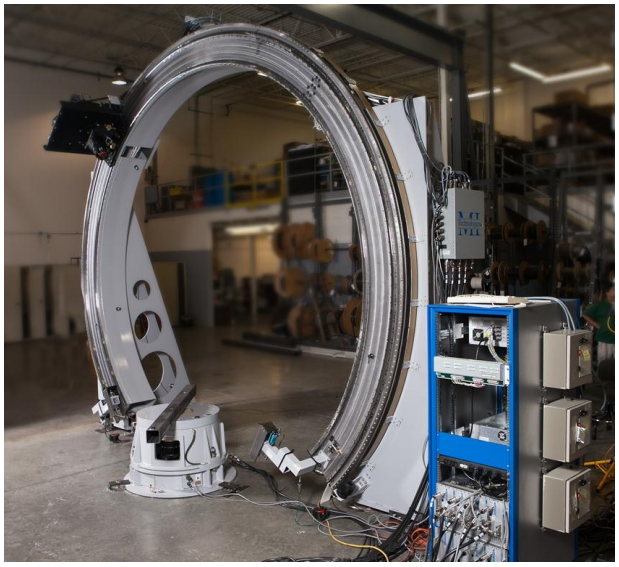

Figure 2 – Photo of System Under Construction

2. Coordinate System

The coordinate system used for this SNF measurement system is shown in Figure 3. The figure shows a view looking down on the measurement system from the positive Z-axis. The azimuth (Phi) axis is installed to be vertical, and defines the Z-axis. The positive X-axis points from the origin to the probe at θ=90°, and Y is approximately the arch (Theta) axis of rotation. The Chi axis, defined by rotation of the probe, is chosen such that Chi-Z is chosen positive toward the system coordinate origin. Chi-Y is parallel to system Y, and Chi-X is defined by the right hand rule.

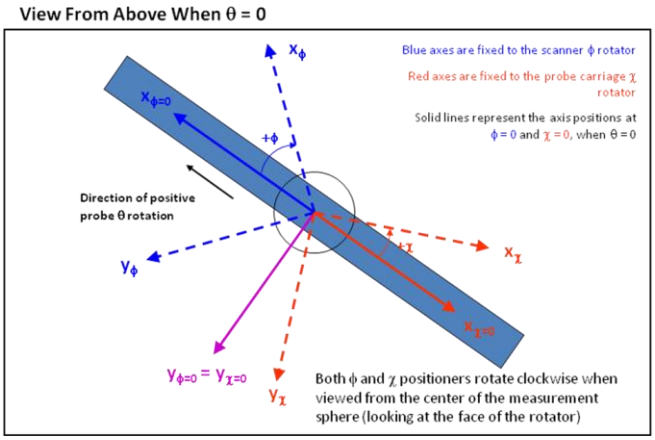

Figure 3 – Coordinate System

3. SNF Positioning System

The motorized four-axis spherical near field scanner consists of a precision azimuth positioner and a high accuracy three-axis probe / arch positioner along with associated motor drives and control units. The probe is mounted on a roll-over-radial slide positioner that is installed on a carriage that moves the probe along the arch. The precision arch establishes the scanner's Theta axis which intersects and is orthogonal to the vertical azimuth axis. The probe's radial and roll axes are aligned to assure that the probe's axis always intersects the measurement sphere's center, i.e., the intersection of the Phi and Theta axes for all theta angles. See Figure 4 for a side view of the positioning system.

To design this high-accuracy positioning system, several key components were considered; the arch (Theta axis), the azimuth rotator (Phi axis) and probe rotator (Chi Axis).

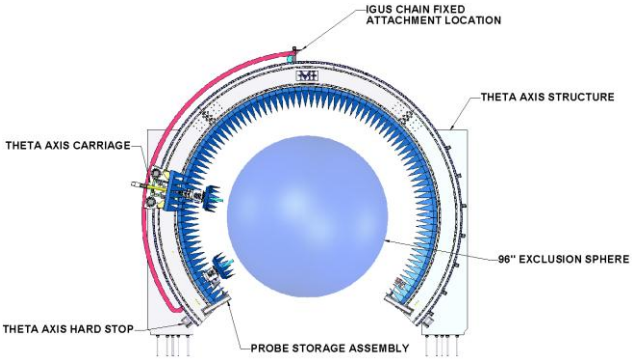

Figure 4 – Side View of Measurement System Showing Measurement Sphere

Arch Positioner (Theta)

The arch is designed and constructed out of three weldments and has a precision mounting surface for mounting precision ground curvilinear rails to carry the probe carriage over a total travel range of +/- 135°.

The rails are mounted to a ground structural ring and are aligned with a laser tracking system. The drive mechanism is a torque-biased, curved rack and pinion system that eliminates backlash by biasing a secondary drive pinion against the primary drive pinion. This results in deterministic, repeatable positioning.

Due to the stationary nature of the arch structure, any gravitational load applied by the probe carriage over its travel range results in very small deflections of the probe position. The arch incorporates a high resolution linear tape encoder for position feedback of the probe in the Theta axis. Because measurement of the Theta axis is conducted at the arch radius rather than at the probe radius, angular accuracy of the probe is significantly better. A high-accuracy, 3 micron repeatability proximity switch is used to initialize the location of the positioner upon start-up. The probe carriage itself is fairly small and lightweight (approximately 100 lbs.) allowing good controllability, aiding in the ability to meet a 5 second re-positioning settling time for a 1 degree step.

Azimuth Rotator (Phi)

The Phi axis uses another dual drive system with a torque bias unit to eliminate backlash, an axial mounted dual read-head encoder to ensure accuracy and a reverse bend cable management chain to effectively manage cables. A key requirement driving the choice of a direct drive and axial mounted encoder was the need of the system to rapidly step and settle within a commanded 1 degree in 1 second. Precision pre-loaded bearings with tight specifications for radial and axial run out were utilized to ensure accuracy under load. The AUT interface to the turntable uses a kinematic mount to achieve alignment repeatability and stability.

Probe Rotation (Chi)

The complex positioner's primary purpose is to accurately locate the phase center of the probe on the measurement grid. As the probe is rotated, a key requirement is that the probe phase center stays fixed on the Chi axis. Probe polarization is achieved using a direct drive positioner. The travel range is -135° to +135°. The polarization positioner is mounted on the linear positioner carriage. The direct drive positioner utilizes a brushless motor with a high accuracy encoder directly coupled to the motor for accuracy and repeatability concerns. A high-accuracy proximity switch is used to initialize the location of the positioner upon start-up.

Measurement Radius (R)

The probe polarization motor is supported by a linear positioner to achieve a 10 cm radial adjustment. The positioner incorporates precision linear guides with a pre-loaded, ground ball screw drive. The ball screw is driven directly by a servo motor incorporating an optical encoder for position feedback. Error compensation of the radial adjustment axis can be used to achieve +/-.00254 cm RMS radial accuracy. A high accuracy proximity switch is used to initialize the location of the positioner upon start-up.

Radius as a Function of Theta {R (Θ)}

The two primary moving axes, Theta and Phi are individually corrected using a static error map measured using a tracking laser interferometer. Each axis is measured throughout its range of travel; residual position errors are calculated and fed back into the position control subsystem for use in error compensation during the antenna measurement.

As the final step in the alignment and calibration process, the position of the probe phase center versus theta travel is compensated. During the measurement of the Theta-axis to determine Theta angular error compensation, the position of the probe aperture is measured using a probe simulator [5]. Errors in the range length are determined and an error map is loaded into the position control subsystem for range length compensation during the antenna measurement.

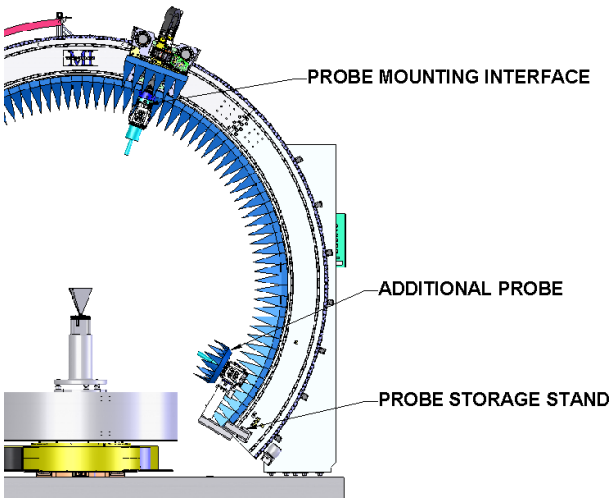

Figure 5 – Probe Changer Detail View

Automatic Probe Changing

The system incorporates a feed changer for fully automated interchange of two probes. See Figure 5 for a detail view of the probe change mechanism. The system utilizes the Theta, Chi and Radial axes positioners for exchange of the probes. No additional axes are required to implement this feature. The feed changer eliminates the

need for multiple redundant servo axes that would be required for a system utilizing multiple probe carriers. Proximity switches are incorporated to detect probe storage and prohibit interference between probes. The design assures that there are no risks of probe collision during the operation of the system.

Efficient automatic feed changing is achieved using blind mate connectors with a repeatable kinematic mounting interface.

The carriage incorporates a reverse bend radius cable chain to manage the necessary RF and drive cables over the Theta travel range

4. Alignment Analysis Example

To achieve the desired 3 dimensional global positioning accuracy the system must be precisely aligned in all of its axes to meet aggressive orthogonality, intersection and pointing requirements. The alignment process involved an iterative series of measurements, data analysis and adjustments. The sequence of adjustments was an important factor to consider due to interrelationships among axes. The following is presented as an example of the many insights exercised to identify sources of error from analysis of measurement data and adjust for them without adversely affecting other alignments.

Figure 6a shows the probe mount Normal Vector Pointing Error as a function of travel along the arch (Theta). This error is the angular deviation of a normal vector originating from the probe mounting surface and intersecting the origin. Trace 1 on the plot shows the total magnitude of the pointing error. The plot shows the 3D error to be above the desired 0.02° through most of the travel. Trace 2 on the plot shows the 2D (Out-of-Plane) error magnitude component of the error calculated from the data.

Analysis of the data reveals that the 2D (Out-of-Plane) error is within the desired 0.02° but it is riding on top of a bias of about 0.02°. Further analysis reveals that the Out-of-Plane error is essentially equal to the bias seen in the 3D error. With this insight, error sources were investigated as to what might be causing the Out-of-Plane error. It was deduced that a rotated polarization axis of about 0.02° could result in this type of Out-of-Plane error.

The polarization axis was subsequently shimmed to remove this rotation resulting in the measurements shown in Figure 6b. Trace 2 now shows the Out-of-Plane error to be well within 0.02° and the 3D error mostly within 0.02° throughout the Theta travel except for two specific spots at theta = 45 and 75 degrees. The plots clearly show the error to be primarily In-Plane error. Therefore the next step in the sequence is to adjust the Theta rails slightly at only these two spots. This was an important conclusion. Over aggressive adjustment of the Theta rails based on the original 3D data would have resulted in large adverse effects to other aspects of the alignment.

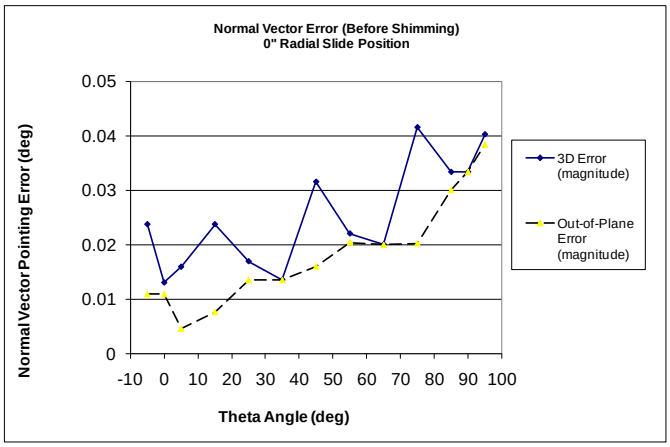

Figure 6a – Normal Vector Pointing Error Before Shimming

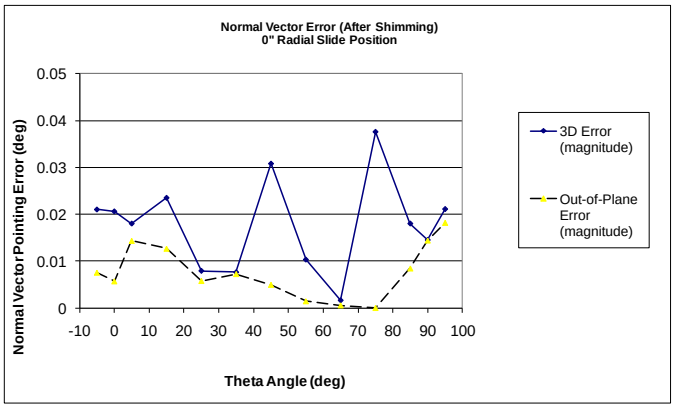

Figure 6b – Normal Vector Pointing Error After Shimming

5. Alignment Results

Figure 7 shows two sets of measured radial position data as a function of Theta position. The mean has been removed from the data leaving only the deviations from the mean plotted. One set of data (consisting of two traces taken in different directions of travel) represents the residual radial error prior to position data correction, labeled “Uncorrected Scans”. The other two traces of data show the residual radial error after using the automated correction feature of the position controller, labeled “Corrected Scans”. The trace labeled “Correction Table” is the set of errors from an earlier calibration measurement used to adjust the motion of the “Corrected Scans”.

While the uncorrected residual error approaches .02 centimeters (.008 inches), using the correction feature of the position controller, the positioning system is usually able to hold the radial dimension within +/- 0.00254 cm (0.001") with the carriage in motion.

Another key performance factor can be seen in Figure 7. The data indicates that the shape of the arch is repeatable and stable over time and direction of travel. The data shown in Figure 7 was taken on different days and in different directions while scanning continuously along the Theta axis.

While the data is not shown in this paper, both the Theta and Phi axes are corrected for residual errors as well. Indicated position of the Theta axis is corrected as a function of residual errors in Theta and the Phi axis is corrected for residual errors in Phi.

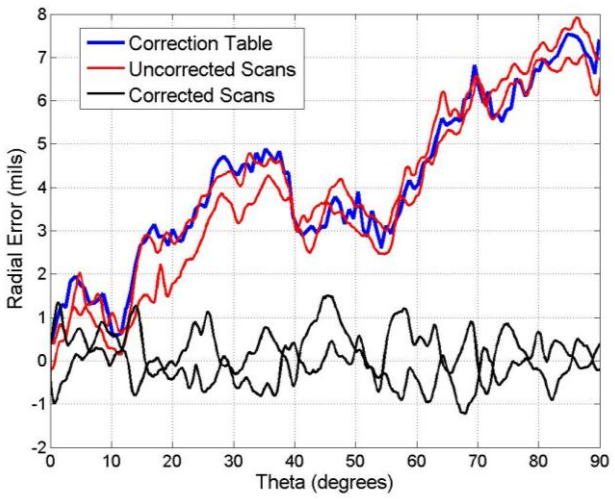

Figure 7 – Residual Radial Errors Before and After Position Correction

6. SNF Measurement System Positioning Accuracy

After final alignment and calibration of each system axis of the SNF measurement system, the performance is shown in Table 1. Performance of the system for parameters that are a function of multiple axes is shown in Table 2.

Table 1: Scanner Axis Positioning Performance

Characteristic	*Performance*			
	Axis			
	Phi	**Theta**	**Chi**	**Radial**
Achieved Step Motion Compensated Position Accuracy	0.0043° RMS	0.0034° RMS	0.01° RMS	0.0079 cm RMS
Readout Resolution	0.0005°	0.0005°	0.0005°	0.00127 cm
Static Readout Stability	+/- 0.0005°	+/- 0.0005°	+/- 0.0005°	+/- 0.00127 cm
Continuous Motion Speed	4 deg/sec	0.9 deg/sec	NA	NA
Step Motion Speed	1 deg. Step in <= 1 second	1 deg. Step in <= 5 second	NA	NA
Load Capacity	1000 kg	NA	9.1 kg	NA

Table 2: Scanner Performance

Characteristic	Performance
Measurement System Radius	150.0 cm +/- 5.1 cm
Probe Mount Normal Vector Alignment	0.039 deg
Non-Intersection of Phi and Theta Axes	0.0053 cm
Orthogonality of Phi and Theta Axes	90 +/- 0.0005 deg
Probe Rotational Alignment	.01 deg RMS

7. Conclusions

A highly-accurate Spherical Near-Field scanner has been designed and constructed to enable characterization of antennas with demanding requirements. Throughout the design the strategy mitigated risk by providing adjustment capability for fine tuning alignment and accuracy as necessary. Each axis was carefully designed using the best techniques available. The Theta axis used precision ground curvilinear rails mounted to a precision ground structural ring that was aligned during installation, and a torque-biased curved rack and pinion drive system to achieve required accuracy with zero backlash. The Phi axis used a torque-bias drive system to achieve zero backlash, and dual axial mounted encoders to ensure accuracy and a reverse bend cable management chain to effectively manage cables. Both the AUT and probe interfaces used kinematic mounts to achieve alignment repeatability and stability.

The primary axes of motion, Theta and Phi were individually calibrated and compensated for angular errors using a tracking laser interferometer to achieve the best angular positioning possible in addition to optical encoders. Once the individual axes were compensated, further position correction was accomplished to correct for residual errors in the radius of the measurement system as a function of Theta.

8. References

[1] Hansen, J.E., ed., Spherical Near-Field Antenna Measurements, London: Peregrinus, 1988.

[2] McBride, S., Marier, J., Kryzak, C., Fordham, J. and Liu, K., "A Large Spherical Near-Field Arch Scanner for Characterizing Low-Frequency Phased Arrays", *AMTA Proceedings*, pp. 71-76, Atlanta, GA, 2010.

[3] Fordham, J., Proctor, J. and Kremer, D., "Precision Positioner Alignment Techniques for Spherical Near Field Antenna Measurements Using Laser Alignment Tools", *AMTA Proceedings*, pp. 317-320, Philadelphia, PA, 2000.

[4] Pierce, S. and Baggett, M., "An Efficient and Highly Accurate Technique for Periodic Planar Scanner Calibration with the Antenna Under Test in Situ", *AMTA Meeting & Symposium*, pp. 543-548, Atlanta, GA, 2004.

[5] Pierce, S. and Langston, J., "Implementation of a Geometric-Error Correction System for Extremely High Probe Position Accuracy in Spherical Near-Field Scanning", *AMTA Meeting & Symposium*, pp. 93-97, Atlanta, GA, 2004.